UNIVERSIDADE ESTADUAL DE MARINGÁ

CENTRO DE CIÊNCIAS BIOLÓGICAS

PROGRAMA DE PÓS-GRADUAÇÃO EM CIÊNCIAS BIOLÓGICAS

ÁREA DE CONCENTRAÇÃO EM BIOLOGIA CELULAR E MOLECULAR

RENATA BUFOLLO RODRIGUES

Dithiothreitol Decreases Oxidative Stress and Cell Death In Ultraviolet-A-Irradiated L929 Fibroblasts

Maringá

2021

RENATA BUFOLLO RODRIGUES

Dithiothreitol Decreases Oxidative Stress and Cell Death In Ultraviolet-A-Irradiated L929 Fibroblasts

Dissertação apresentada ao Programa de Pós-Graduação em Ciências Biológicas (área de concentração – Biologia Celular e Molecular), da Universidade Estadual de Maringá para a obtenção do grau de Mestre em Ciências Biológicas.

Orientador: Prof. Dr. Celso Vataru Nakamura

Maringá

2021

Dados Internacionais de Catalogação-na-Publicação (CIP)
(Biblioteca Central - UEM, Maringá - PR, Brasil)

R696d

Rodrigues, Renata Bufollo

Dithiothreitol decreases oxidative stress and cell death in ultraviolet-a-irradiated l929 fibroblasts / Renata Bufollo Rodrigues. -- Maringá, PR, 2021.

36 f.: il. color., figs., tabs.

Orientador: Prof. Dr. Celso Vataru Nakamura.

Dissertação (Mestrado) - Universidade Estadual de Maringá, Centro de Ciências Biológicas, Departamento de Biologia, Programa de Pós-Graduação em Ciências Biológicas (Biologia Celular), 2021.

1. Peroxidação lipídica. 2. Espécie reativas de oxigênio. 3. Radiação ultravioleta. 4. Fotoquimioprotetor. 5. Fibroblastos dérmicos. I. Nakamura, Celso Vataru, orient. II. Universidade Estadual de Maringá. Centro de Ciências Biológicas. Departamento de Biologia. Programa de Pós-Graduação em Ciências Biológicas (Biologia Celular). III. Título.

CDD 23.ed. 571.6

Rosana de Souza Costa de Oliveira - 9/1366

FOLHA DE APROVAÇÃO

RENATA BUFOLLO RODRIGUES

Dithiothreitol Decreases Oxidative Stress and Cell Death In Ultraviolet-A-Irradiated L929 Fibroblasts

Dissertação apresentada ao Programa de Pós-Graduação em Ciências Biológicas (área de concentração – Biologia Celular e Molecular), da Universidade Estadual de Maringá para a obtenção do grau de Mestre em Ciências Biológicas.

Aprovado em: 28 de abril de 2021.

COMISSÃO JULGADORA

Prof. Dr. Celso Vataru Nakamura

Universidade Estadual de Maringá (Presidente)

Profª. Drª. Anacharis Babeto de Sá Nakanishi

Universidade Estadual de Maringá

Profª. Drª. Sueli de Oliveira Silva Lautenschlager

Universidade Estadual de Maringá (Presidente)

BIOGRAFIA

Nascida em 9 de março de 1997, em Maringá, Paraná, Renata Bufollo Rodrigues é filha de Dileusa Batista da Silva e Marcos Bufollo Rodrigues. Concluiu o ensino fundamental em 2011, no Colégio Mater Dei e o ensino médio em 2014, no Instituto de Educação Estadual de Maringá. Em 2015 ingressou na Universidade Estadual de Maringá onde formou-se Bacharel em Bioquímica no ano de 2019. Neste mesmo ano iniciou o mestrado pelo Programa de Pós-Graduação em Ciências Biológicas, na Universidade Estadual de Maringá, ao qual apresenta dissertação para obtenção do grau de mestre, com enfoque no teste de substâncias para fotoproteção de células da pele.

AGRADECIMENTO

Á minha mãe, Dileusa Batista da Silva, que sempre esteve ao meu lado ensinando sobre valores morais e éticos, além de ter me educado para resistir sob qualquer adversidade. Á minha avó, Irene Antônia Gomes, agradeço por ter me criado a seu exemplo de mulher determinada, resiliente e independente. Ao meu irmão de coração, Peterson Ribeiro, agradeço pela paciência, constância, e apoio incondicional. Aos demais familiares, pelo apoio e energias positivas.

Às minhas amigas Cler Jansen e Daniele Zanzarin, que me acompanham desde a graduação, sempre me incentivando a fazer o melhor. Aos meus amigos de laboratório, especialmente a pós-doutora Thaysa Ksiaskiewcz Karam, a doutora Mariana Maciel de Oliveira, aos doutorandos Karine Campos Nunes, Karina Miyuki Retamiro, Bruna Terra Alves da Silva, Elisa Parcero Hernandes e Rodolfo Bento Balbinot e as mestrandas Rayanne Regina Beltrame Machado e Amanda Beatriz Kawano Bakoshi por seus incontáveis conselhos, suporte emocional e prático e disposição durante os dois anos de mestrado.

Aos professores responsáveis por transferir conhecimento da melhor maneira durante o mestrado, especialmente a meu orientador, Prof. Dr. Celso Vataru Nakamura, por sua dedicação a pesquisa e confiança em meu potencial, bem como disposição e abertura para novas ideias e incentivo rumo ao novo, o despertar da curiosidade.

Por fim agradeço a Universidade Estadual de Maringá, a todos os membros do Departamento de Ciências Biológicas e ao Programa de Pós-Graduação em Ciências Biológicas, por possibilitarem a realização desta dissertação. Aos órgãos de fomento Conselho Nacional de Desenvolvimento Científico e Tecnológico (CNPq), Coordenação de Aperfeiçoamento Pessoal de Nível Superior (CAPES), Fundação Araucária e Fundo de Financiamento de Estudos de Projetos e Programas (FINEP) por financiamento estudantil fornecido.

APRESENTAÇÃO

Esta dissertação é composta por um resumo geral, em português e inglês, e um artigo científico contemplando resultados, em grande parte, obtidos durante o mestrado. Este artigo descreve a atividade fotoprotetora do ditiotreitol frente a radiação UV-A, sob fibroblastos dérmicos. Deverá ser submetido para publicação ao Journal of Photochemistry and Photobiology B: Biology, cujo fator de impacto é de 4.383 (Qualis CBI – A1).

RESUMO GERAL

A UV-A (400-315 nm) faz parte dos comprimentos de onda emitidos pela radiação ultravioleta (UV) da luz solar. É a maior contribuinte para o envelhecimento extrínseco da pele por inviabilizar fibroblastos dérmicos, responsáveis por produzir fibras elásticas e de colágeno. Intracelularmente, a exposição a UV-A pode levar a produção exacerbada de espécies reativas de oxigênio (ERO's), que interage com biomoléculas para se estabilizar, ocasionando peroxidação lipídica, dissipação do potencial de membrana mitocondrial ($\Delta\psi m$), redução na produção de ATP, condensação do DNA e sobrecarga do sistema antioxidante endógeno, conduzindo a célula ao estresse oxidativo e até a morte celular.

Estudos prévios determinaram que o ditiotreitol (DTT) é capaz de neutralizar os radicais livres 2,2-azinobis-3-etilbenzotiazolina-6-ácido sulfônico ($ABTS^{\bullet+}$), 2,2-difenil-1-picrilhidrazil ($DPPH^{\bullet}$), ânion superóxido ($O2^{\bullet-}$) e redução do íon férrico (Fe^{3+}). Além disso, o pré-tratamento de fibroblastos L929 por 1 hora, com 50 e 100 µM de DTT, evitou parte da inviabilização das células irradiadas (20 J/cm^2), diminuiu o conteúdo de ERO's e a peroxidação lipídica. Este artigo reúne os resultados acima citados, obtidos durante a graduação e experimentos seguintes realizados durante o mestrado, a fim de comprovar a capacidade do DTT em diminuir o estresse oxidativo e a morte celular.

A radiação UV-A diminuiu a atividade de SOD, CAT e a concentração de GSH sendo o DTT capaz de reestabelecer parte de suas atividades enzimáticas, mas não a concentração de GSH. Não houve alteração na concentração de grupamentos tióis com a irradiação. UV-A também induziu a produção de peróxido de hidrogênio (H_2O_2), reduziu o $\Delta\psi m$ e provocou condensação do DNA, revertidos pelo pré-tratamento com DTT. ATP foi diminuído por UV-A, mas DTT não foi capaz de reverter tal depleção. A morte celular dos fibroblastos L929 irradiados com UV-A se deu tanto por necrose quanto por apoptose tardia e DTT foi capaz de evitá-las parcialmente. Desta maneira, pode-se concluir que o DTT é fotoquimioprotetor e possui perfil promissor quanto a prevenção de danos à saúde da pele provocada por UV-A, como o envelhecimento extrínseco, por reduzir o estresse oxidativo provocado pelas ERO's e a morte celular por necrose e apoptose tardia.

PALAVRAS-CHAVE: polióI, radiação ultravioleta, espécies reativas de oxigé necrose, apoptose, fotoquimioproteção.

ABSTRACT

UV-A (400-315 nm) is part of the wavelengths emitted sunlight ultraviolet radiation (UV). It is the most contributes extrinsic skin aging, as it makes dermal fibroblasts unfeasible, responsible for the production of elastic fibers and collagen. Intracellularly, exposure to UV-A can lead to the exacerbated production of reactive oxygen species (ROS), which interact with other biomolecules, causing lipid peroxidation, dissipation of the mitochondrial membrane potential ($\Delta\psi m$), reduction in ATP production, DNA condensation and overload of the endogenous antioxidant system, leading the cell to oxidative stress and even cell death.

Previous studies have determined that dithiothreitol (DTT) is able to neutralize free radicals 2,2-azinobis-3-ethylbenzothiazoline-6-sulfonic acid ($ABTS^{\bullet+}$), 2,2-diphenyl-1-picrilhidrazil ($DPPH^{\bullet}$), anion superoxide ($O2^{\bullet-}$) and ferric ion (Fe^{3+}). In addition, the pre-treatment of L929 fibroblasts for 1 hour, with 50 and 100 μM of DTT, avoided part of the unviable of irradiated cells (20 J/cm^2), in addition to reducing the excessive production of ROS and lipid peroxidation. This article gathers the results mentioned above, obtained during the graduation and following experiments carried out during the master's degree, with the objective of proving the ability of DTT to reduce oxidative stress and cell death.

UV-A radiation decreased the activity of SOD, CAT and the concentration of GSH. DTT was able to restore part of its enzymatic activities, but not the concentration of GSH. There was no change in the concentration of thiol groups with radiation. UV-A also induced the production of hydrogen peroxide (H_2O_2), reduced $\Delta\psi m$ and caused DNA condensation, reversed by pre-treatment with DTT. ATP was decreased by UV-A, but DTT did not reverse this depletion. Cell death of L929 fibroblasts irradiated with UV-A was due to late apoptosis and necrosis, and DTT was able to partially avoid them. Thus, it can be concluded that DTT is photochemoprotector and has a promising profile in terms of preventing damage to skin health caused by UV-A, such as extrinsic aging, by reducing oxidative stress caused by ROS and cell death.

KEYWORDS: Polyol, ultraviolet radiation, reactive oxygen species, necrosis, apoptosis, photochemoprotection.

SUMÁRIO

Dithiothreitol Decreases Oxidative Stress and Cell Death in Ultraviolet-A-Irradiated L929 Fibroblasts

Renata Bufollo Rodrigues[a], Mariana Maciel de Oliveira[b], Tânia Ueda-Nakamura[b], Sueli de Oliveira Silva Lautenschlager[b], Celso Vataru Nakamura[a,b,*].

a. Biological Sciences Pos-graduation Program, Maringá State University, Maringá, Brazil;
b. Pharmaceutical Sciences Pos-graduation Program, Maringá State University, Maringá, Brazil.

*Corresponding author at: Maringá State University, Av. Colombo, n. 5790, Zona 7, CEP: 87020-900, Maringá, Paraná, Brazil. Email-address: cvnakamura@uem.br (C. V. Nakamura).

Abstract

The Ultraviolet-A (UV-A) radiation, present in sunlight, can lead to cell oxidative stress by excessive production of reactive oxygen species (ROS), causing death by necrosis and apoptosis, compromising skin health. Dithiothreitol (DTT) was chosen for present great capacity to neutralize free radicals 2,2-azinobis-3-ethylbenzothiazoline-6-sulphonic acid ($ABTS^{\bullet+}$), 2,2-diphenyl-1-picrylhydrazyl ($DPPH^{\bullet}$), superoxide anion ($O2^{\bullet-}$) at xanthine oxidase (XOD) assay and to reduce ferric ion (Fe^{3+}) to ferrous ion (Fe^{2+}) at Ferric Reducing Antioxidant Power (FRAP) assay. This article evaluated induced damage to dermis cells, L929 fibroblasts, after UV-A radiation and found that DTT (50 and 100 µM) increased fibroblasts cell viability compared to irradiated cells, in a neutral red (NR) assay, reduced intracellular ROS production, including hydrogen peroxide (H_2O_2), lipid peroxidation, alteration in mitochondrial membrane potential ($\Delta\psi m$) and DNA condensation, reducing oxidative stress. DTT also improve the endogenous antioxidant system of cells by increasing activity of enzymes superoxide dismutase (SOD) and catalase (CAT), depleted in UV-A irradiated cells. Besides, reduced necrosis and apoptosis was observed in L929 fibroblasts UV-A irradiated after treatment with DTT. These results showed that DTT is promising in the prevention of skin photoaging and photodamage induced by UV-A for promotes photochemoprotection against the harmful effects of this radiation, reducing oxidative stress and cell death due to its antioxidant capacity.

Keywords

Polyol, ultraviolet radiation, reactive oxygen species, necrosis, apoptosis, photochemoprotection.

1. Introduction

Human skin is an important physical barrier against external damaging agents, including solar radiation that can promote injuries in this organ. In addition to protecting the integrity of internal organs, it allows the individual to experience sensations, synthesize vitamin D and establish homeostasis, being important to keep it healthy. In the dermis are located fibroblasts, a cell type that produce extracellular matrix and are involved in wound healing due to their ability to release growth factors [1,2].

Ultraviolet radiation (UV) from sunlight is divided into three wavelengths (λ): UV-A (400-315 nm), UV-B (315-280 nm) and UV-C (280-100 nm). UV-C has a greater harmful potential, but it is almost completely filtered by the ozone layer. Approximately 5% of the UV that reaches planet Earth is UV-B, which reaches the epidermis and the upper part of the dermis. The remaining 95% are comprised by UV-A, which is less energetic, permeating even the dermis, where it exerts profound changes in the connective tissue. The concern with exposure to UV-A is due to its constant intensity during the day, being little affected by the variation of latitude, season, climatic conditions, thickness of the ozone layer and time of exposure. In addition, UV-A can overtake glass, cotton in clothing and reach the retina of the eye, increasing the skin's exposure to this radiation [3,4,5].

The main effect of exposure to UV-A is the exacerbated production of reactive oxygen species (ROS) including hydrogen peroxide (H_2O_2) and superoxide anion ($O_2^{\bullet-}$) [5,6]. In the search for stabilization, ROS interact with biomolecules, such as nuclear and mitochondrial DNA, causing ruptures, and membrane lipids, leading to lipid peroxidation, which contributes to their ruptures that influence their selective permeability, loss of mitochondrial membrane potential ($\Delta\psi m$), leading to a reduction at adenosine triphosphate (ATP) production [5,7]. The excess of ROS overloads the endogenous antioxidant system, reducing the concentration of reduced glutathione (GSH) and decreasing the activity of superoxide dismutase (SOD) and catalase (CAT). This set of events can lead to cell oxidative stress, which can induce cell death by apoptosis and necrosis. UV-A radiation also is the main responsible for extrinsic aging due to the degradation of collagen and elastin, the main proteins of the extracellular matrix produced by fibroblasts, promoting loss of strength and elasticity [3,8].

Although widely used as a protective measure against sunburn, photoaging, and skin cancer, the use of sunscreens can have undesirable consequences and may not be completely effective in protecting against harmful effects of UV. Due to the dependence of UV-B for the production of vitamin D3, there is evidence that the use of sunscreens can reduce its synthesis since its objective is to absorb or repel such radiation. Especially against UV-A radiation, common sunscreens are not as effective. Thus, it is necessary to use substances, such as antioxidants, capable of acting mainly on the ROS produced by UV-A, neutralizing them and reducing their harmful effects [6,9,10].

Dithiothreitol (DTT), a synthetic molecule with high antioxidant activity, capable of maintaining reduced thiol groups and reducing the photo hemolysis of erythrocytes irradiated at 400 nm was chosen to have its photochemoprotective effect determined, on L929 dermal fibroblasts irradiated with UV-A, since no article proposed such an approach. DTT chemical structure is in figure 1 and present the thiol and hydroxyl groups which give reducing properties to DTT, in addition to providing stability to enzymes [11,12]. DTT acts as a reducer by reducing disulfide bonds to free sulfhydryl groups in proteins, forming a six-membered ring. It redox potential is -0.33V at pH 7.0 [13]. The effects resulting from the radiation exposure were evaluated, mainly those related to the production of ROS. Therefore, the present study aimed to determine the photochemical protection path offered by DTT, exploring the oxidative stress caused by ROS overproduced and cell death that UV-A promotes.

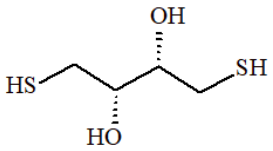

Figure 1. Chemical structure of DTT.

2. Materials and Methods

2.1 Evaluation of Antioxidant Capacity of DTT in Cell Free Assays

2.1.1 $ABTS^{\bullet+}$ Assay

DTT and Ascorbic Acid (AA, both Sigma-Aldrich® Corporation, St. Louis, MO, USA, used as a control because it is an antioxidant widely used in photochemoprotection) were evaluated for their ability to neutralize the 2,2'-

azino-bis-3-ethylbenzothiazolin-6-sulfonic cationic radical ($ABTS^{\bullet+}$, 7 mM), formed after mixing with potassium persulfate (140 mM) for 16 h. The ability of substances to donate hydrogens to the $ABTS^{\bullet+}$ was evaluated. Trolox was used as a standard antioxidant for the preparation of a calibration curve. The $ABTS^{\bullet+}$ solution was then diluted in ethyl alcohol to an absorbance of 0.70 ± 0.05 nm at 734 nm, observed on a BIO-TEK Power Wave XS microplate reader. DTT and AA were diluted in ethanol at concentrations of 10,4167 at 1,3017 µg/mL. Subsequently, 7 µL of each sample was mixed with 200 µL $ABTS^{\bullet+}$ in a clear 96-well plate, followed by reading at 734 nm. A 4-4000 µM 6-hydroxy-2,5,7,8-tetramethylchroman-2-carboxylic acid ethanolic solution (Trolox, Sigma-Aldrich® Corporation, St. Louis, MO, USA) was used for the calibration curve (y = -0.0163x + 0.6664; r = 0.999) and the results were expressed in µmol Trolox Equivalent (TE)/g sample [14].

2.1.2 $DPPH^{\bullet}$ Assay

DTT and AA were evaluated for electron donation to the 2,2-diphenyl-1-picrylhydrazyl radical ($DPPH^{\bullet}$, Sigma-Aldrich® Corporation, St. Louis, MO, USA). They were diluted in methanol at concentrations of 3, 5, 7, 9 and 11 µg/mL and 100 µL of each was mixed with 100 µL of $DPPH^{\bullet}$ diluted in methanol (130 µM) in a transparent 96-well microplate. The negative control was made using 100 µL of $DPPH^{\bullet}$ solution and 100 µL of methanol. After 30 min incubation at room temperature and in the dark, the plate was read on a Power Wave XS BIO-TEK microplate reader at 517 nm. The percentage inhibition of the $DPPH^{\bullet}$ radical was obtained by the equation: % inhibition = $(A_{nc}-A_s)/A_{nc}$ x 100, where A_{nc} is the negative control absorbance ($DPPH^{\bullet}$ in methanol) and A_s the $DPPH^{\bullet}$ absorbance in the presence of samples. The sample concentration capable of inhibiting 50% (IC_{50}) of the $DPPH^{\bullet}$ radical was calculated by linear regression. This methodology was first described by Blois [15], but used with modifications, like protocol performed by Oliveira et al. [16].

2.1.3 FRAP Assay

For the Ferric Reducing Antioxidant Power (FRAP) assay, DTT and AA were evaluated for the ability to donate electrons to ferric ion (Fe3+), reducing to ferrous ion (Fe2+) when it receives electrons from the compound with a redox potential below 0.7 V [16]. For this, an acetate buffer solution (0.3 mM at pH 3.6), 2,4,6-tripyridyl-s-triazine (TPTZ, Sigma-Aldrich® Corporation, St. Louis, MO, USA, 10 mM in 40 mM HCl) and iron chloride hexahydrate (20 mM), 1:1:10 v/v was prepared and remained at 37 °C for 30 min [17]. DTT and AA were diluted in methanol (10.4167 to 1.3017 µg/mL) and 30 µL of each solution was mixed with 150 µL of the Fe^{3+} containing solution in a transparent 96-well plate and read after 30 min incubation (37

°C) at 593 nm on a Power Wave XS model BIO-TEK microplate reader. The negative control was made by adding 30 µL of the sample-free ethanol and 150 µL of the solution to the well. Trolox ethanolic solution with different concentrations (4-4000 µM) was used to obtain the calibration curve (y = 0.0797x + 0.3582; r = 0.997) and results expressed in µmol TE/g of sample [20].

2.1.4 XOD Assay

To determine the ability of DTT and AA to neutralize the superoxide anion ($O_2^{\bullet-}$), a radical produced when xanthine oxidase (XOD) converts hypoxanthine to xanthine [21], a serial dilution of the substances was made in 50% ethanol: water (29,851 to 2,174 µg/mL). A reaction solution was prepared in eppendorf-like microtubes containing 400 µL glycine buffer (0.1 mol/L containing 1 mol/L EDTA, pH 9.4), 150 µL xanthine (6 mmol/L), and 10 µL of luminol (0.06 mmol/L), plus 10 µL of each dilution of the prepared sample. Then the tubes received 100 µL of xanthine oxidase solution (20 mU/mL) and it was vortexed for 30 s, applied to a white 96-well microplate, and immediately read on a SpectraMax L Microplate Reader, Molecular Devices. The negative control was performed by adding 10 µL of 50% ethanol/water without the presence of samples. The IC_{50} was obtained by the following equation: % inhibition = $(C_{nc} - C_s)/C_{nc}$ x 100, where C_{nc} is the chemioluminescence observed in the negative control and C_s is presented by one of the samples [20].

2.2 Cell Culture, treatment and UV-A Irradiation

NCTC clone L929 murine fibroblasts (ATCC® CCL1™) were aseptically cultured in screw-capped plastic bottles containing Modified Eagle Dulbecco Medium (DMEM, Life Technologies/Gibco Laboratories, Grand Island, NE, USA) supplemented with 2 mM L -glutamine, 10% fetal bovine serum (SFB, Life Technologies/Gibco Laboratories, Grand Island, NE, USA), and 1% antibiotic containing streptomycin sulfate (50 µg/mL) and penicillin (50 IU/mL) at 37 ºC, 5% CO_2 and 95% humidity.

For plating, when cell culture reached 80% confluent monolayer, cells were detached using trypsin, counted in a Neubauer Chamber under light microscopy, and diluted in supplemented DMEM. According to the experiment to be performed, L929 fibroblasts were added in either 6-well plates (4 x 10^5 cells/mL) or 24 and 96-well plates (2.5 x 10^5 cells/mL). Plates were incubated for 24 h in an oven and then treated.

In all experiments, except for cytotoxicity, pre-treatment prior to irradiation was carried out for 1 h with DTT (50, 100 uM) or N-acetylcysteine (NAC, Sigma-Aldrich® Corporation, St. Louis, MO, USA, 1 mM). In the cytotoxicity assay, treatment was performed for 24 h with only DTT (50,

100 and 500 µM). DTT and NAC was diluted in DMEM not supplemented or Hank's Balanced Saline (HBSS, Sigma-Aldrich, St. Louis, MO, USA).
Then the cells were irradiated with UV-A (20 J/cm^2), an intensity capable of making 50% of L929 fibroblasts unfeasible, it was measured by a VLX-3W Vilber Lourmat radiometer (CX-365 nm) and the plate kept at a fixed distance of 20 cm from the UV-A lamp on an ice plate in a white wooden box. After completion of irradiation, HBSS buffer was replace with serum-free and antibiotic-free DMEM and the cells used for the experiments that follow.

2.3 Determination of Cellular Viability

2.3.1 Cytotoxicity Assay

L929 fibroblasts were plated in transparent 96-well plates, incubated for 24 h, treated with 100 µL DTT at 50, 100 and 500 µM, diluted in DMEM medium for 24 h. Then the cells were washed with 100 µL PBS and 200 µL neutral red solution was added (NR, Interlab, São Paulo, SP, BR, 40 µg/mL) with the plate incubated for 3 h protected from light. NR dye is metabolized by lysosomes of viable cells and produce alterations in absorbance. Afterward, NR was removed and 200 µL of fixative solution (1% $CaCl_2$ and 2% formaldehyde in PBS) were added and incubated for 5 min, and then replaced by a solution composed of ethanol: 50% water and 1% Acetic Acid. After 10 min in the dark, the plate was shaken and read on a Power Wave XS BIO-TEK microplate reader at 540 nm [21].

2.3.2 Cytoprotection Assay

L929 cells were plated in 24-well plates, incubate for 24 h, pre-treated for 1 h with 500 µL DTT at 50 and 100 µM, diluted in HBSS for 1 h. Afterward, cells were washed with 500 µl PBS, added 500 µL HBSS, and exposed to UV-A. HBSS was then replaced by serum-free DMEM, incubated for 24 h, and subjected to the NR assay as described in 2.4.1 [21].

2.3.3 Cell Morphology

The cells plated for the cytoprotection assay were observed under an inverted phase contrast microscope Olympus CKX41, 20x magnification, after being treated and irradiated.

2.4 DTT Assessment Against Oxidative Stress Induced by UV-A

2.4.1 ROS Levels

L929 cells were plated on 96-well black microplates, after 24 h washed with 100 µL of PBS, pre-treated for 1 h with DTT or NAC and then irradiated with UV-A. Immediately after that, cells receiver 5 µL of the 2',7'-dichlorodihydrofluorescein diacetate marker (H_2DCFDA, 10 µM, Eugene, OR, USA) diluted in HBSS, which remained on the cells for 45 min in the dark at 37 ºC. The probe H_2DCF-DA is a non-fluorescent and emits fluorescence when oxidized by intracellular ROS, producing DCF, which can be quantified. The marker was then removed, the wells washed with PBS and 100 µL of HBSS added for quantification of ROS in a Victor X-3 PerkinElmer fluorescence reader at 488 nm excitation and 525 nm emission [22]. Protein concentration was quantified using the Bradfort method (Bio-Rad, CA, USA). Briefly, each of the wells in the 96-well plate received 10 µL of Triton-X (0.2%), were homogenized and 5 µL of each of the lysates was transferred to a new well in a transparent 96-well microplate. After that, 100 µL of the 20% Bradfort solution was added to the samples. Staining intensity was measured in a Power Wave XS Bio-TEK reader at 595 nm. Serial dilution of bovine albumin was used for the calibration curve.

To visualize ROS production, fluorescence microscopy was performed by plating L929 fibroblasts on a round slide in 24-well microplates. The cells were incubated for 24 h, pre-treated for 1 h with DTT or NAC and irradiated with UV-A. After 24 h, the cells were marked with H_2DCFDA (10 µM) for 30 min and kept at 37 ºC in the dark. The wells were washed with PBS and the coverslip poured over a slide containing 3% glycerol for observation under an OLYMPUS BX51 fluorescence microscope using Olympus UC30 camera. A hundred cells were counted for each treatment.

2.4.2 H_2O_2 Levels

L929 cells were plated on 96-well black microplates, after 24 h washed with 100 µL of PBS, pre-treated for 1 h with DTT or NAC and then irradiated with UV-A. Immediately after that, cells receiver 50 µL of the Amplex Red and Horseradish Peroxidase (15 µM and 0.15 U, respectively, Invitrogen, Eugene, OR, USA) diluted in Tris-HCl 0.1 M, pH 7.5, which remained on the cells for 30 min in the dark at room temperature. In the presence of peroxidase, Amplex Red reacts with H_2O_2 and produces resorufin, which can be quantified by fluorescence. The quantification of H_2O_2 was performed in a Victor X-3 PerkinElmer fluorescence reader at 571 nm excitation and 585 nm emission. The assay was did based on the manufacturer's instructions. Protein concentration was quantified using the Bradford method.

2.4.3 Integrity of Endogenous Antioxidant System

To evaluate the ability of the endogenous antioxidant system of L929 fibroblasts to neutralize ROS, the activity of the enzymes SOD and CAT, the levels of GSH and thiol group were measured [16,23]. L929 fibroblasts were

added in 6-well microplates, pre-treated for 1h with DTT or NAC and irradiated with UV-A. Then a cell lysate was prepared by washing the cells with cold PBS, dropping them from the plate by scraping with a cell scraper in cold tris-HCl buffer (10 mM pH = 7.4) and collecting them in Eppendorf microtubes. The cells were kept in an ice bath and sonicated for 60 s in a tip sonicator (5 s on, 5 s off and 30% amplitude). Then they received 10% Triton X-100, were incubated on ice for 10 min, centrifuged (14,000 rpm, 10 min and 4 ºC) and the supernatant was collected in another microtube, kept in an ice bath, and subsequently frozen at -80 ºC. Protein dosage was performed using Bradford reagent.

To determine CAT activity, 50 mg of protein from each lysate was added in a quartz cuvette, the volume was made up to 1000 µL with 50 mM potassium phosphate buffer, pH 7.0 and finally 300 µL H_2O_2 was added. The reading on a Shimadzu UV-1700 spectrophotometer at 240 nm was performed every 10 s for 10 min. It's possible quantify the directly activity of CAT agains their It's possible quantify the directly activity of CAT against their substrate H_2O_2.

In the evaluation of SOD activity, 50 mg of protein per cell lysate were mixed until 1000 µL of tris-HCl buffer (200 mM) and EDTA (2 mM) pH 8.2 at 37 ºC, 70 µL of pyrogallol (15 mM, Sigma-Aldrich, St. Louis, MO, USA) in a quartz cuvette. The reading was done on a Shimadzu UV-1700 spectrophotometer at 420 nm every 10 s for 2 min. Pyrogallol used is capable of self-oxidizing in a basic medium and forms $O2^{\bullet-}$ which, in the presence of SOD and EDTA, has its formation reduced [16,24].

To quantify the GSH levels, a serial dilution of the same was prepared to perform a calibration curve. Then, 10 µL of each lysate or GSH was added in a black 96-well microplate, along with 180 µL of 0.1 M sodium phosphate buffer and 5 mM EDTA (pH = 8.0) and 10 µL of O-phthaldialdehyde (OPT, Sigma-Aldrich, St. Louis, MO, USA) at 1 mg/mL diluted in methanol. OPT binds to GSH at pH 8.0, forming a measurable fluorescent complex [4,25,26]. After 15 min of incubation in the dark, the microplate was read in a Victor X-3 PerkinElmer fluorimeter at 350 nm excitation and 420 nm emission.

For determination of thiols groups, 100 µL of each lysate was added in a transparent 96-well microplate, after 100 µL of PBS was added, followed by 10 µL of 5,5'-dithiobis-2-nitrobenzoic acid (DTNB or Ellman's reagent, 1 mM, Thermofisher, Waltham, MA, USA). In the presence of sulfhydryl groups, DTNB forms TNB2-, which produces a yellow color proportional to the number of thiols and can be quantified by spectrophotometry. The absorbance was read in 432 nm in a microplate reader Power Wave XS Bio-TEK [27].

2.5 Evaluation of DTT Against UV-A-Induced Biomolecule Damage

2.5.1 Occurrence of Lipid Peroxidation

L929 cells were plated on 96-well black microplates, after 24 h washed with 100 µL of PBS, pre-treated for 1 h with DTT, NAC or H_2O_2 (1 mM, positive control, data not shown) and then irradiated with UV-A. After that, cells were incubated for 24 h with incomplete DMEM. On the next day, the cells receiver 100 µL of HBSS and above it, 10 µL of the diphenyl-1-pyrenylphosphine (DPPP, 20 µM, Invitrogen, Eugene, OR, USA) diluted in HBSS, which remained on the cells for 30 min in the dark at 37 ºC. DPPP was used, which reacts with lipid hydroperoxides and produces fluorescence [28]. The marker was then removed, the wells washed with PBS and 100 µL of HBSS added for quantification of lipid peroxidation in a Victor X-3 PerkinElmer fluorescence reader at 351 nm excitation and 460 nm emission. Protein concentration was quantified using the Bradford method [29].

2.5.2 Alterations in Mitochondrial Membrane Potential

L929 fibroblasts were plated in black 96-well microplates, pre-treated for 1 h with DTT or NAC, irradiated with UV-A and incubated for 24 h. Then a positive control was performed using Carbonyl Cyanidine m-chlorophenylhydrazone (CCCP, 100 µM, data not shown), incubated on the cells for 30 min. In each of the wells, 100 µL of Tetramethylrhodamine Ethyl Ester (TMRE, Molecular Probes, Eugene, OR, USA) was added to 0.025 µM for 30 min, the plate being kept in the dark, in an oven at 37 ºC and 5% CO_2. The positively charged TMRE is able to permeate the cell and accumulate in active mitochondria, whose charge is negative, emitting red fluorescence. When $\Delta\psi m$ is depolarized, TMRE does not accumulate correctly in the mitochondria and causes changes in fluorescence, which can be quantified [30,31].Then the plate was read on a Victor X-3 PerkinElmer fluorimeter at 540/595 nm excitation and emission, respectively [27]. Protein dosage was performed using the Bradfort method.

2.5.3 Alterations in ATP levels

L929 fibroblasts were plated in white 96-well microplates, pre-treated for 1 h with DTT or NAC, irradiated with UV-A, the HBSS was removed and 100 µL of PBS was added. After 30 min at room temperature, 50 µL of CellTiter-Glo (Promega, WI, USA) was added and the plate was shaken for 2 min in a plate shaker. In this assay, the CellTiter-Glo kit was used, which has luciferin, converted to luciferase by ATP, luminescent and capable of quantification. After 10 min, the luminescence was read on SpectraMax L Microplate Reader, Molecular Devices. The assay was performed based on manufacturer's instructions.

2.5.4 Determination of DNA Condensation

Fluorescence microscopy was performed by plating L929 fibroblasts on a round slide in 24-well microplates. The cells were incubated for 24 h, pre-treated for 1 h with DTT or NAC and irradiated with UV-A. After 24 h, the cells were marked with Hoechst 33342 (Invitrogen, Eugene, OR, USA, 8 µM) for 15 min and kept at 37 ºC in the dark. Hoechst marker 33342 is capable of binding to dsDNA and promoting fluorescence. The wells were washed with PBS and the coverslip poured over a slide containing 3% glycerol for observation under an OLYMPUS BX51 fluorescence microscope. A hundred cells were counted for each treatment [23].

2.6 Application of DTT Against Apoptosis and Necrosis Induced by UV-A

2.6.1 Determination of Cell Death Stages

Round coverslips were inserted into 24-well plates and L929 fibroblasts were plated on them. Cells were pre-treated for 1 h with DTT or NAC and UV-A irradiated. On the third day, the wells were washed with PBS, marked with acridine orange (Sigma-Aldrich, St. Louis, MO, USA) and propidium iodide (Invitrogen, Eugene, OR, USA), both at 1 µg/mL and kept for 10 min in the dark. After this time, the wells were washed with PBS, the coverslip was removed from the plate and poured over a rectangular slide containing 10 µL of 3% glycerol. The fluorescence observation was made using an OLYMPUS BX51 fluorescence microscope. A hundred cells were counted for each treatment [32].

In the assay using acridine orange, which is a fluorescent marker and capable to intercalated with nucleic acids, it is possible to differentiate viable cells (green nucleus, marked only with AO), necrotic cells (red nucleus, marked only with PI), and cells in late apoptotic (marked with AO and PI, whose overlapping of the markers promotes orange color) [16,27].

2.6.2 Determination of Apoptosis and Necrosis

L929 fibroblasts was plated in a 6-well microplate and after 24 h pre-treated for 1 h with DTT or NAC and irradiated with UV-A. After another 24 h, released from the plate in enzyme-free PBS dissociation buffer (Life Technologies/Gibco Laboratories, Grand Island, NY, USA) washed in 0.25% HBSS and EDTA, resuspended in 500 µL of binding buffer containing 140 mM NaCl, 5 mM $CaCl_2$ and 10 mM HEPES-Na at pH 7.4. Then the cells received 2 µL of Annexin V - Fluorescein isocyanate (FITC) (Invitrogen, Eugene, OR, USA) and it was incubated for 15 min in the dark at room temperature. Finally, 50 µL of propidium iodide (PI, Invitrogen, Eugene, OR, USA, 2 µg/ml) was added. After this period, a flow cytometer reading was performed, acquiring 30,000 events in a flow cytometer (Becton

Dickinson, FACSCalibur). The data were analyzed using the CellQuest software [16].

Annexin V-FITC + PI assay is able to differentiate cells in initial apoptosis, necrosis and apoptosis plus necrosis. Apoptotic cells transport phosphatidylserine from the inner part of the cell membrane to the outer part [33], and Annexin V can conjugate to phosphatidylserine and promote fluorescence. PI marks necrotic cells, which allows the entry of this marker when the integrity of the cell membrane is compromised. Apoptotic and necrotic cells have double labeling [16].

2.7 Statistical Analysis

Data are shown as mean ± standard deviation (SD) for three independent experiments. The statistical significance of the differences between groups was assessed using a unilateral analysis of variance (ANOVA) followed by the Tukey test, in Prism 5.0 software. Values of $p < 0.05$ were considered statistically significant.

3. Results and Discussion

Antioxidant substances are extremely important for skin photochemoprotection, as they are able to neutralize ROS, molecules intensely produced when cells are exposed to UV, especially UV-A [34]. When in a state of homeostasis, ROS are important in common biochemical reactions, however in excess, ROS obtain stabilization by reacting with biomolecules, which can lead to generalized oxidative stress, characterized by peroxidation of membrane lipids, alteration in $\Delta\psi m$, depletion of endogenous antioxidants, damage to DNA, among others, contributing greatly to photoaging and even photocarcinogenesis [4,5,7,35]. The use of DTT, an antioxidant capable of donating electrons and hydrogens to other molecules and reducing protein disulfide bonds, maintaining its structure and function [36], may be able to photochemoprotect cells, being used as a pre-treatment.

The antioxidant property of DTT, as already reported in the literature [11,36], was confirmed through the antioxidant tests *in vitro* $ABTS^{\bullet+}$, $DPPH^{\bullet}$, FRAP and $O_2^{\bullet-}$. According to Table 1, DTT was able to donate hydrogen to $ABTS^{\bullet+}$, showing a value of 7,13 µM TE/µM, significantly higher than the result found for ascorbic acid (AA), it is

5.70 µM TE/µM, thus being more efficient than AA in neutralizing $ABTS^{\bullet+}$, since came closer to Trolox standard.

The DTT showed an inhibitory concentration of half of the radicals (IC_{50}) $DPPH^{\bullet}$ of 39.80 µM. This is due to its performance as a reducing agent, due to the disulfide bonds present in its molecule (Figure 1), being able to donate electrons to $DPPH^{\bullet}$. AA used as a standard has a high antioxidant activity, with an IC_{50} of 37.19 ± 0.07 µM.

Regarding the FRAP test, Table 1 shows that DTT was able to donate electrons to Fe^{3+}, obtaining a value of 5.82 µM TE/µM. A similar value was obtained for AA (8.22 µM TE/µM). At pH 7.0, the redox potential for DTT is -0.33 V, while for AA it is 0.35 V [13,37], both smaller than the potential of the TPTZ complex, thus being able to reduce the Fe^{3+} present in it because electrons flow from compounds with the lowest redox potential to the one with the highest redox potential.

In the XOD assay (Table 1), it is possible to observe that DTT was able to neutralize $O_2^{\bullet-}$. The IC_{50} value obtained for the DTT was 27.94 µM, significantly higher than IC_{50} of AA (12.66 µM). DTT is a polyol, and a similar test was carried out with other polyols, such as erythritol, xylitol, sorbitol and mannitol, showing that this class of compounds has, in fact, the ability to neutralize $O_2^{\bullet-}$, in addition to determining that the number of hydroxyls is directly proportional to the ability to neutralize it [38]. This result is linked to that AA, which has more hydroxyls than DTT, showed better antioxidant performance in this assay.

Together, these results prove the antioxidant capacity of DTT in cell-free assays, turning DTT a good candidate to protect cells irradiated with UV-A against harmful effects from excessive ROS production. Then, assay with cells were conducted.

Due to the ability of UV-A radiation to reach and exert its deleterious effects on the cells present in the dermis, fibroblasts were chosen for the next experimental design, since this is the main cell type residing in this layer. The maintenance of its integrity is essential for the health of the skin, as it produces an extracellular matrix, which mainly comprises elastic and collagen fibers, giving elasticity and strength to the skin [6,39].

Table 1. Antioxidant capacity of DTT at *in vitro* assays

Sample	**$ABTS^{\bullet+}$ (µM TE/ µM)**	**$DPPH^{\bullet}$ IC_{50} (µM)**	**FRAP (µM TE/ µM)**	**$O_2^{-\bullet}$ IC_{50} (µM)**
DTT	7.13 ± 0.30***	39.80 ± 0.08	5.82 ± 0.18	27.94 ± 0.32***

AA	5.70 ± 0.83	37.19 ± 0.07	8.22 ± 2.63	12.66 ± 0.44

Results expressed as mean ± SD (n = 3). Significant differences between Dithiotreithol (DTT) and Ascorbic Acid (AA) averages performed by Tukey test (*** p <0.001). IC_{50}: 50% inhibitory concentration; TE: Trolox Equivalents.

In the cytotoxicity assay (Figure 2A), different concentrations of DTT (50, 100 and 500 µM) were tested, which remained for 24 h under L929 fibroblasts. None of them were toxic to the cells, as they did not alter the viability of L929 fibroblasts in relation to the negative control, of untreated cells, considered as 100% viability.

Regarding cytoprotection (Figure 2B), the fibroblasts were irradiated with UV-A dose of 20 J/cm^2, determined to be capable of reduce 50% of cell viability. A pre-treatment (before irradiation) for 1 h was performed using the three concentrations of non-cytotoxic DTT and a concentration of NAC (1 mM). NAC is an antioxidant that, according to the literature, is capable of protecting fibroblasts directly against damage caused by UV-A, reducing DNA damage and neutralizing ROS, in addition to donating cysteine for the synthesis of GSH [33]. It is possible to observe that there was no dose-dependence for the tested DTT concentrations, where the dose of 50 µM leads to 79%, 100 µM to 76%, and 500 µM to 60% of cell viability. Only 50 and 100 µM protected the cells significantly when compared to the positive control (irradiated and untreated cells), and these concentrations were chosen for the subsequent experiments. Cells treated with NAC showed 65% cell viability.

The photoprotection of the lowest dose of DTT can be explained by the facilitated permeation in the cell. In large quantities, DTT can form aggregates with each other, where its two hydroxyls form hydrogen bonds, and its two sulfhydryl, disulfide bonds, depending on factors such as pH, ions and heavy metals. When in lower concentration, DTT interactions are likely to occur more with the extracellular medium, composed of different molecules, including hydrophilic ones, such as water, than between the molecules of the DTT itself. Such inferences are based on the principles of chemical interactions and concepts of biochemistry, which deal with the osmotic homeostasis of a cell. [41].

The cells used in the cytoprotection assay were visualized under optical microscopy (Figure 2C). It is possible to observe that UV-A reduced the amount of L929 fibroblasts present, caused rounding, and cell spacing, compared to the negative

control (non-irradiated and untreated cells), where they have defined format, closed monolayer, enlarged and flattened shape. Both concentrations of DTT, as well as NAC, were able to maintain this monolayer, avoiding the loss of morphology presented by cells irradiated with UV-A, confirming that the pre-treatment with DTT has the ability to protect L929 fibroblasts.

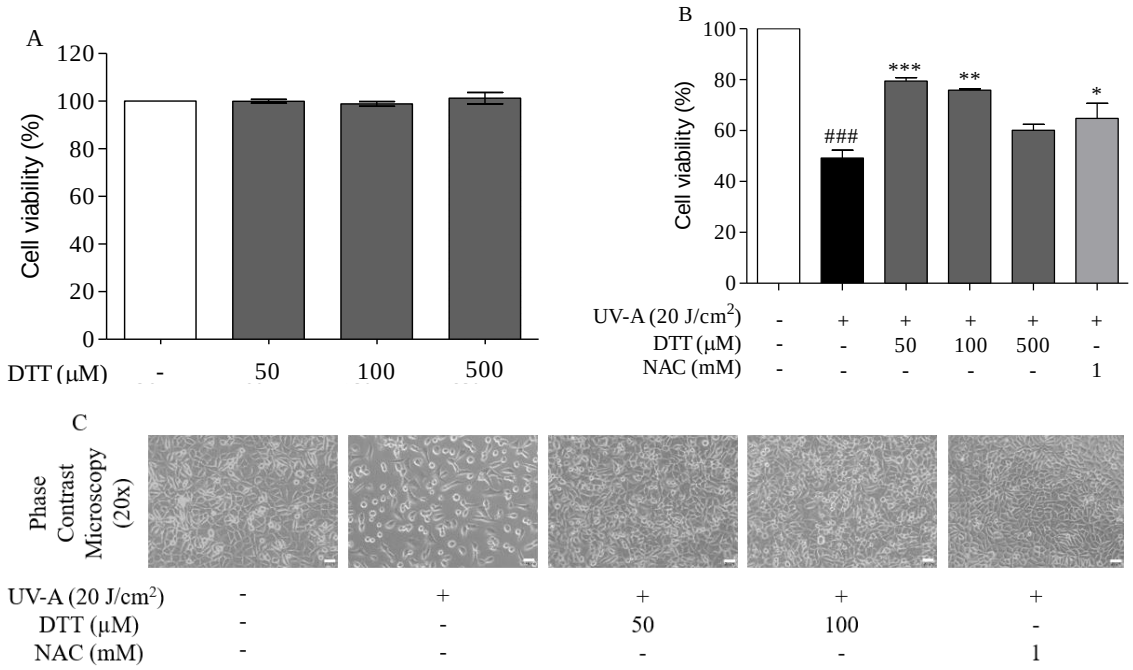

Figure 2. Effect of treatment with DTT on cell viability (A and B) and morphology (C) of L929 fibroblasts. A: Cytotoxicity after 24 h of DTT treatment assessed by the neutral red method; B: Cytoprotection after pre-treatment for 1 h with DTT or NAC and UV-A irradiation (20 J/cm^2) assessed by the neutral red method. Each column represents the mean ± SD (n = 3). ### ($p < 0.001$) indicates a significant difference compared to non-irradiated cells (white columns). *, ** and *** ($p < 0.05$, 0.01 and 0.001, respectively) indicates a significant difference compared to cells irradiated with UV-A (black column) only. C: Phase contrast microscopy to assess cell morphology after UV-A irradiation (20 J/cm^2) and pre-treatment for 1 h with DTT or NAC. Each image represents three different experiments. Scale bars: 20 μm.

Oxidative stress can promote cells death, whose redox imbalance caused by excess of ROS, the main photoproduct of UV-A exposure, induces damage to biomolecules, which can initiate necrosis processes and apoptosis. The predominance of oxidizing species is of great concern since the effects on the skin can accelerate the extrinsic aging process, as well as leading to cases of inflammation and even skin cancer [6,10,42]. Secondary markers were used to determine the level of cellular oxidative stress, such as those for the content of ROS and H_2O_2.

Figure 3A shows that negative control cells showed baseline values of ROS (71 Fluorescence Units/µg of protein), whereas cells only irradiated with UV-A showed a significant increase (1074 Fluorescence Units/µg of protein) than negative control. Both concentrations of DTT (50 and 100 µM) and the NAC standard (1 mM) significantly reduced this content compared to cells irradiated with UV-A (39%, 40% and 39%, respectively). Under fluorescence microscopy (Figure 3C), it is possible to observe the low fluorescence of non-irradiated cells, its increase in cells irradiated with UV-A, indicating an increase in ROS, and a significant ROS reduction in cells irradiated with UV-A and treated with DTT and NAC, proving the results obtained through quantification.

Figure 3B shown H_2O_2 levels. The basal quantity of the production of this molecule (866 Fluorescence Units/µg of protein) was quite high with UV-A irradiation (increased H_2O_2 by 200%), and treatments, with both DTT and NAC were able to reduce this exacerbated production (71% and 73%, respectively). This is mainly due to the antioxidant properties of the substances used, which can neutralize H_2O_2, a molecule capable of inducing protein oxidation and intrinsic apoptosis [5,30].

Together, these results allow us to infer that DTT may be able to reduce harmful effects of ROS excessively produced by exposure to UV-A radiation, such as lipid peroxidation, DNA damage (breaks and condensation), the overload of the endogenous antioxidant system and even cell death. Therefore, the following trials focused on these analyses.

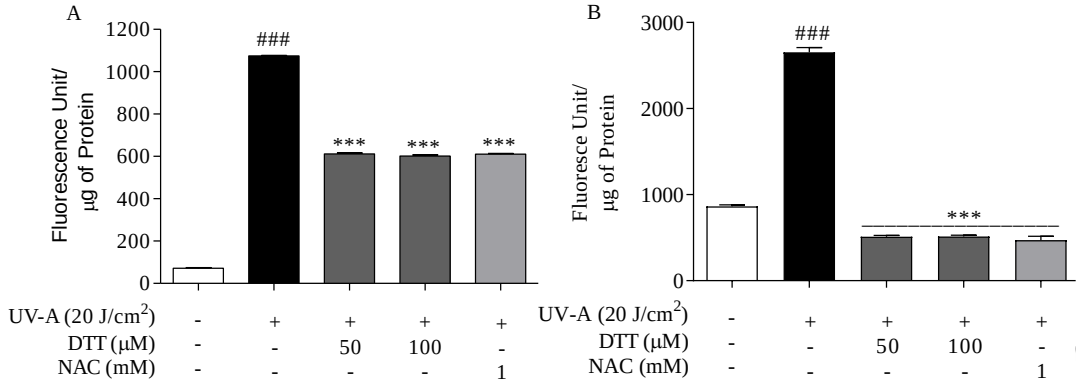

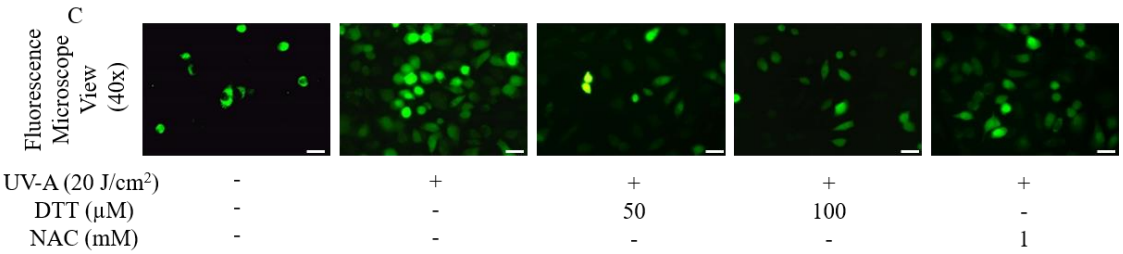

Figure 3. Effect of UV-A radiation (20 J/cm^2) and pre-treatment for 1 h with DTT on ROS production (A and C) and H_2O_2 production (B) of L929 fibroblasts. A: ROS content evaluated by quantification of fluorescent probe H_2DCF-DA and Bradfort protein assay; B: Evaluation of H_2O_2 content by quantification of fluorescent of Resorufin and Bradfort protein assay. Each column represents the mean ± SD (n = 3). ### ($p < 0.001$) indicates a significant difference compared to non-irradiated cells (white columns). *** ($p < 0.001$) indicates a significant difference compared to cells irradiated with UV-A (black columns) only. C: ROS production evaluated for observation of fluorescent probe H_2DCF-DA in fluorescence microscopy. Each image represents three different experiments. Scale bars: 100 µm.

Exogenous antioxidants are important to neutralize ROS, and also to assist endogenous antioxidants in their role in combating oxidative stress, since UV-A radiation can reduce their activities, such as CAT, SOD and the concentration of the GSH molecule [4,6]. Thus, we analyzed how the pre-treatment with DTT and NAC could reflect on the activity of these components of the endogenous antioxidant system, when under UV-A irradiation.

CAT is the enzyme responsible for decomposing H_2O_2 into H_2O and O_2, essential in the neutralization of this ROS, reducing the reactivity of H_2O_2 on biomolecules. [43,44]. In Figure 4A it is possible to observe that, as expected, UV-A reduced the enzyme activity (by 42%) compared to non-irradiated cells of increase of activity. Pre-treatment with DTT was able to increase its quantity. The concentration of 100 µM of DTT was significantly different from the irradiated control (32%). It is evident that the DTT, in the highest concentration, in addition to neutralizing the excessive production of H_2O_2 (Figure 3B), is still able to assist part of the restoration of CAT activity, providing additional support to combat this ROS.

Figure 4B shows the results for SOD activity, an enzyme capable of converting $O_2^{\bullet-}$ into O_2 and H_2O_2 [16,24]. The results were expressed at unity of SOD, concentration capable to neutralize $O_2^{\bullet-}$. UV-A reduced the activity of this enzyme by 75% compared to non-irradiated cells. The treatments with DTT at 50 and 100 µM almost normalize the activity of this enzyme (70% and 73%, respectively), in relation to the UV-A irradiated cells. NAC also supported the activity of the SOD (reversed its activity by 70%). This result is quite important, as DTT, in addition to allowing SOD to

carry out its activity of converting $O_2^{\bullet-}$ into other products, preventing the spread of lipoperoxidation, for example, still guarantees partial CAT activity, which culminates in neutralizing H_2O_2.

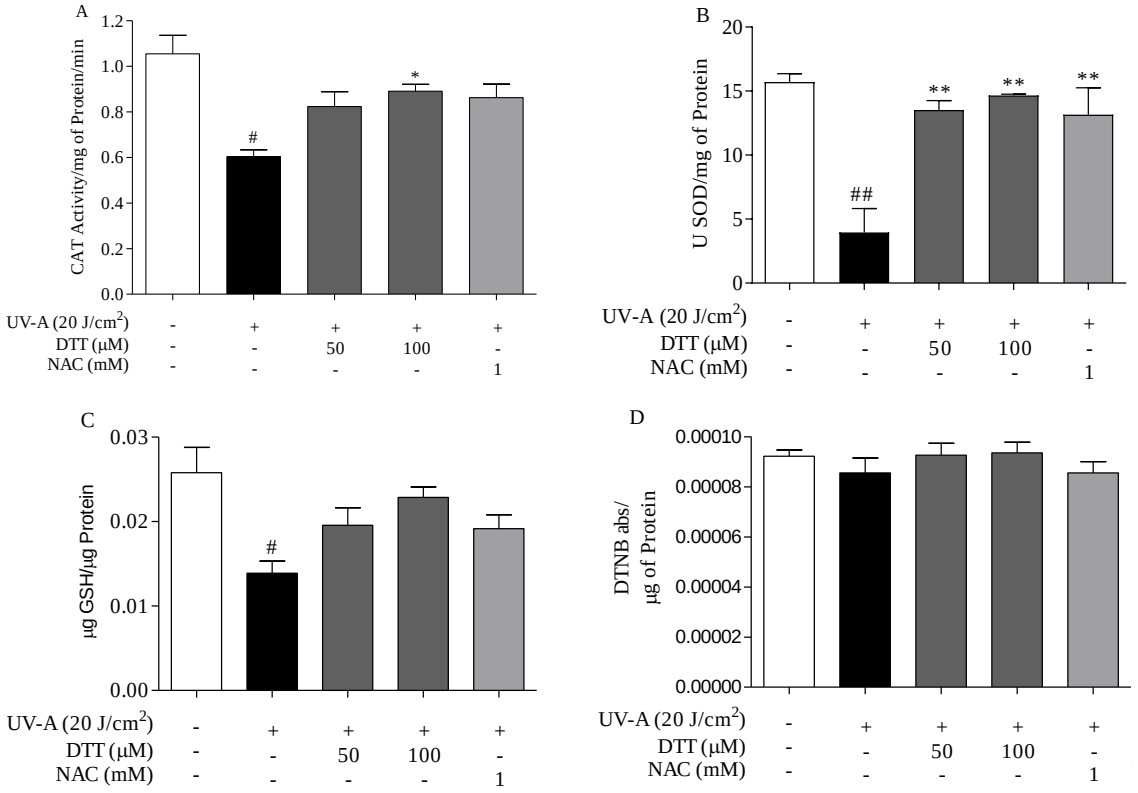

Figure 4. Effect of UV-A radiation (20 J/cm^2) and pre-treatment for 1 h with DTT on endogenous antioxidant system of L929 fibroblasts. A: Catalase activity (CAT) assessed by H_2O_2 consumption; B: Superoxide dismutase (SOD) assessed by pyrogallol oxidation; C: Reduced glutathione level (GSH) quantified using O-phtaldialdehyde fluorescence; D: Thiol groups levels quantified using Ellman's reagent. Each column represents the mean ± SD (n = 3). # and ## ($p < 0.05$ and 0.01, respectively) indicates a significant difference compared to non-irradiated cells (white columns). * and ** ($p < 0.05$ and $p < 0.01$, respectively) indicates a significant difference compared to cells irradiated with UV-A (black columns) only.

The endogenous antioxidant system is composed of enzymatic and non-enzymatic molecules, GSH is the most abundant non-enzymatic molecule, acting in the neutralization of ROS and lipid hydroperoxides, in addition to regenerating enzymes such as glutathione peroxidase (which in turn neutralizes H_2O_2). This molecule is essential to maintain the cell's redox state, especially under oxidative stress, however, UV-A radiation can reduce its concentration. In this experiment [4,25,26]. Figure 4C shows that UV-A decreases the concentration of this molecule in the cell by 47% compared to the non-irradiated cells. 50 and 100 μM of DTT and 1 mM of NAC were

not significantly different from the control irradiated with UV-A (30%, 40% and 28%, respectively).

GSH is a type of cellular antioxidant based on thiol, but there are numerous proteins, such as glutathione peroxidase and glutathione-s-transferase, so it is interesting to quantify the levels of this group [42]. In Figure 4D, it is possible to observe that UV-A radiation does not significantly influence the presence of thiols, reducing only 8% of its concentration compared to the non-irradiated control. DTT and NAC were not significantly different from non-irradiated control or control irradiated with UV-A.

These results indicate that UV-A decrease the endogenous antioxidant system, and DTT protect part of this reduction by promotes the maintenance of a general redox state in the cell, due to its proven ability to donate electrons and hydrogens to free radicals, due to the presence of the -SH and -OH groups of its molecule (Figure 1).

When the endogenous antioxidant system isn't able to maintain cell redox homeostasis, the oxidative stress is established, and excessive ROS can lead to damage to cell membranes, including via the intrinsic apoptosis pathway, which causes the appearance of pores in the external mitochondrial membrane, causing the $\Delta\psi m$ to be dissipated [30,31]. As expected, UV-A reduced the $\Delta\psi m$ by 33% compared to the non-irradiated control. Both concentrations of DTT, 50 and 100 µM, led to a partial reestablishment of this potential in a significant way, as well as the tested NAC concentration (24%, 30% and 24%, respectively), compared to the irradiated control (Figure 5A).

Associated with the loss of $\Delta\psi m$ is the reduction or halt in the production of ATP, an important energy molecule in cellular survival, used in several metabolic processes [45]. In Figure 5B it can be seen that UV-A significantly reduced the levels of ATP compared to non-irradiated control (55%). DTT and NAC did not promote a significant reestablishment of this molecule.

Loss of $\Delta\psi m$ and reduction in ATP levels are characteristic effects of both death by necrosis and apoptosis. In necrosis, there is no need for ATP, unlike apoptosis, which needs this energetic molecule to proceed. Changes in $\Delta\psi m$ indicate the occurrence of intrinsic apoptosis, where there is the release of cytochrome c to cytosol, a pro-apoptotic factor. [5,7,25].

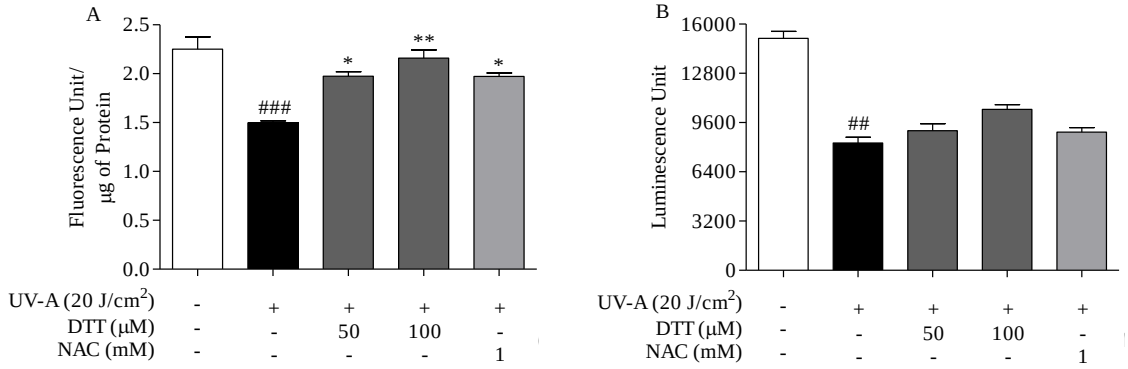

Figure 5. Effect of UV-A radiation (20 J/cm^2) and pre-treatment for 1 h with DTT on the potential of mitochondrial membrane (A) and ATP levels (B) of L929 fibroblasts. A: Evaluation of mitochondrial membrane potential by quantifying Tetramethylrhodamine Ethyl Ester fluorescence and Bradfort protein assay; B: Evaluation of ATP levels by quantifying the luminescence of the CellTiter-Glo. Each column represents the mean ± SD (n = 3). ## and ### ($p < 0.01$ and $p < 0.001$, respectively) indicates a significant difference compared to non- irradiated cells (white columns). * and ** ($p < 0.05$ and $p < 0.01$, respectively), indicates a significant difference compared to cells irradiated with UV-A (black columns) only.

Knowing that ROS can lead to lipid peroxidation Figure 6A makes it evident that this irradiation promotes lipoperoxidation, as it raised basal levels of non-irradiated control by 263%. Pre-treatments with DTT at 50 and at 100 µM were able to significantly reduce lipoperoxidation (36% and 33%, respectively), compared to irradiated control. NAC also protected against lipoperoxidation (30% compared to irradiated cells).

Phospholipid membranes can directly absorb UV, as well as having their polyunsaturated fatty acid hydrogens removed by ROS, such as hypochlorous acid, forming a peroxyl radical, which reacts with other lipids and forms unstable products, causing a series of cascade reactions, called lipoperoxidation [30,46]. Peroxidized biomembranes suffer from loss of selectivity, allowing for the indiscriminate entry and exit of compounds, including ROS, which can contribute to cellular redox imbalance and even death [46]. DTT was able to reduce lipid peroxidation as well as reduce ROS, helping to reduce oxidative stress as a whole, promoted by UV-A irradiation.

Excess ROS, as well as UV-A directly can induce DNA damage. Apoptotic characteristic, the exacerbated condensation in DNA can be visualized. The greater the condensation, the greater its intensity [16,31]. It is possible to observe a quantitative and qualitative increase in DNA condensation promoted by UV-A irradiation on L929 fibroblasts (Figures 6B and C, respectively), from baseline levels (1.33%) to significant condensation (18%). Both concentrations of DTT greatly reduced this condensation,

with 50 and 100 µM showing only 5.33% condensation, while NAC was particularly less efficient in protecting this harmful mechanism, with condensation of 12.33%.

Figure 6C clearly shown that fluorescence is increased in cells only irradiated with UV-A compared to non-irradiated cells, and the reduction in fluorescence with pre-treatment, especially with DTT. These results are particularly important, as both lipid peroxidation, which can lead to damage to biological membranes and consequent loss of selective permeability, and DNA damage, can induce cell death, mainly by apoptosis (damage to DNA) and necrosis (loss integrity), or even necroptosis, where, in the final stages of apoptosis, there may also be a loss of membrane integrity.

The results so far demonstrated that cells irradiated with UV-A can be led to cell death process either by apoptosis or by necrosis, or even by necroptosis. For this reason, the Annexin V-FITC + PI and LA + PI assays were performed, in order to try to conclude how the L929 fibroblasts are being conducted to cell death.

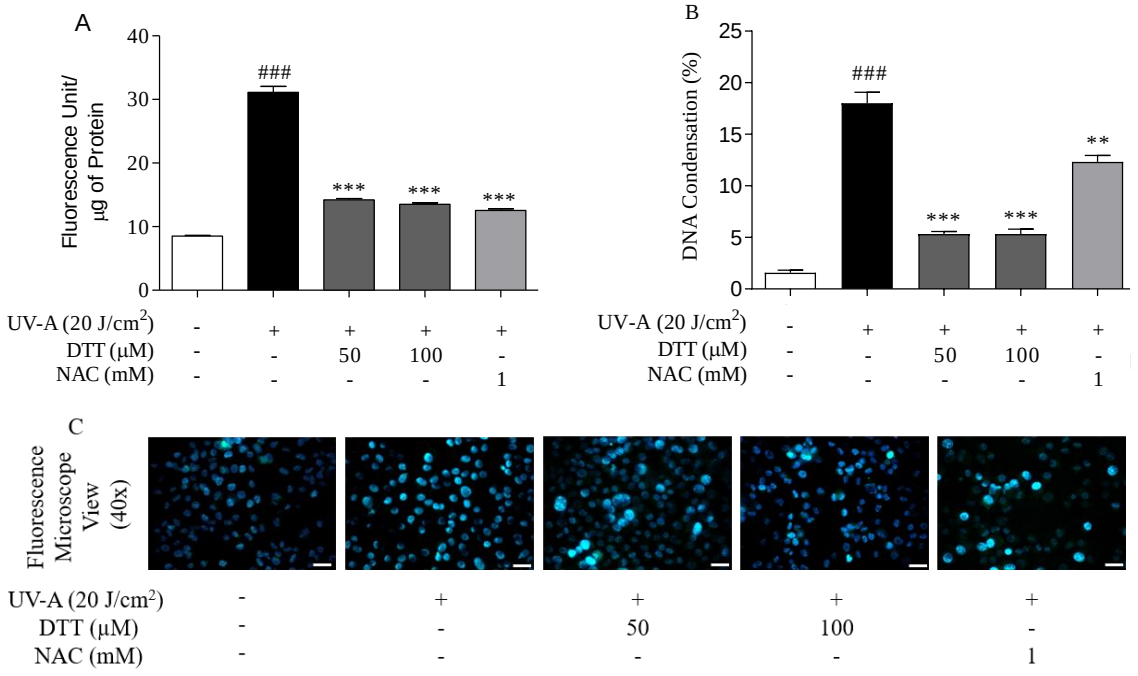

Figure 6. Effect of UV-A radiation (20 J/cm^2) and pre-treatment for 1 h with DTT on lipid peroxidation (A) and DNA condensation (B) of L929 fibroblasts. A: Evaluation of lipid peroxidation production by quantification of fluorescent probe DPPP and Bradfort protein assay; B: DNA condensation evaluated by quantification of fluorescent probe Hoechst 33342. Each column represents the mean ± SD (n = 3). ### ($p < 0.001$) indicates a significant difference compared to non-irradiated cells (white columns). ** and *** ($p < 0.01$ and $p < 0.001$, respectively) indicates a significant difference compared to cells irradiated with UV-A (black columns) only; C: DNA condensation evaluated by observation of fluorescent probe Hoechst 33342 in fluorescence microscopy. Each image represents three different experiments. Scale bars: 100 µm.

In Figure 7A, the raw data from a flow cytometry reading allow us to observe that non-irradiated cells remained in the left and below quadrant, showing most of the cells negative for PI and Annex V-FITC, which indicates they remained viable. However, UV-A irradiation displaced a significant number of cells to the upper left quadrant, positive for PI, that is, inducing cells to a necrotic process. In Figure 7B it is possible to observe that the pre-treatments with 50 and 100 µM DTT were able to decrease approximately 50% the necrosis induced by UV-A, with NAC presenting a very similar result.

Quantitatively (Figure 7A), UV-A reduced cell viability from 92% to 79%. Non-irradiated cells had only 5% of their total in necrosis, while cells irradiated with UV-A increased to 17%. Viable cells in 50 and 100 µM DTT and 1 mM NAC were approximately 87%. DTT reduced the necrosis observed in UV-A, with 50 µM leading to 10%, 100 µM to 11% and 1 mM NAC to 10%. Initial apoptosis and apoptosis plus necrosis did not have significantly different values compared to irradiated and non-irradiated L929 fibroblasts, as well as in the pre-treatments performed.

The experiment using LA + PI (Figure 7C and D) shows that UV-A promoted a reduction in cell viability (88%) and an increase in necrosis (indicated by the arrow, marked only in red) and late apoptosis (indicated by the arrow heads, marked in orange) in 8% and 7%, respectively. Pre-treatment with DTT significantly increased the number of viable cells compared to UV-A irradiated cells to approximately 97% at both concentrations. NAC promoted a significant increase in the number of viable cells (97%).

These results indicate that cells irradiated with UV-A were led to cell death by late apoptosis and necrosis (Figure 8). The main characteristics of death due to apoptosis were observed, being the excess of ROS, including H_2O_2, directly linked to the induction of intrinsic apoptosis, mitochondrial depolarization, caused by the loss of integrity of the external mitochondrial membrane, as well as the chromatin condensation.

The reduction of ATP, a non-essential molecule in necrotic processes, as well as the dissipation of $\Delta\psi m$ and the establishment of oxidative stress due to exposure to UV-A radiation are characteristic of death by necrosis. The hypothesis of necroptosis was discarded, as cytometry did not indicate double marking for necrosis and apoptosis

(Figure 6A), required for necroptosis. This result corroborates articles that indicate that UV-A radiation induces apoptosis [47,48] and also necrosis [48] in certain cell types, including epidermal cells, keratinocytes, and dermal cells, fibroblasts.

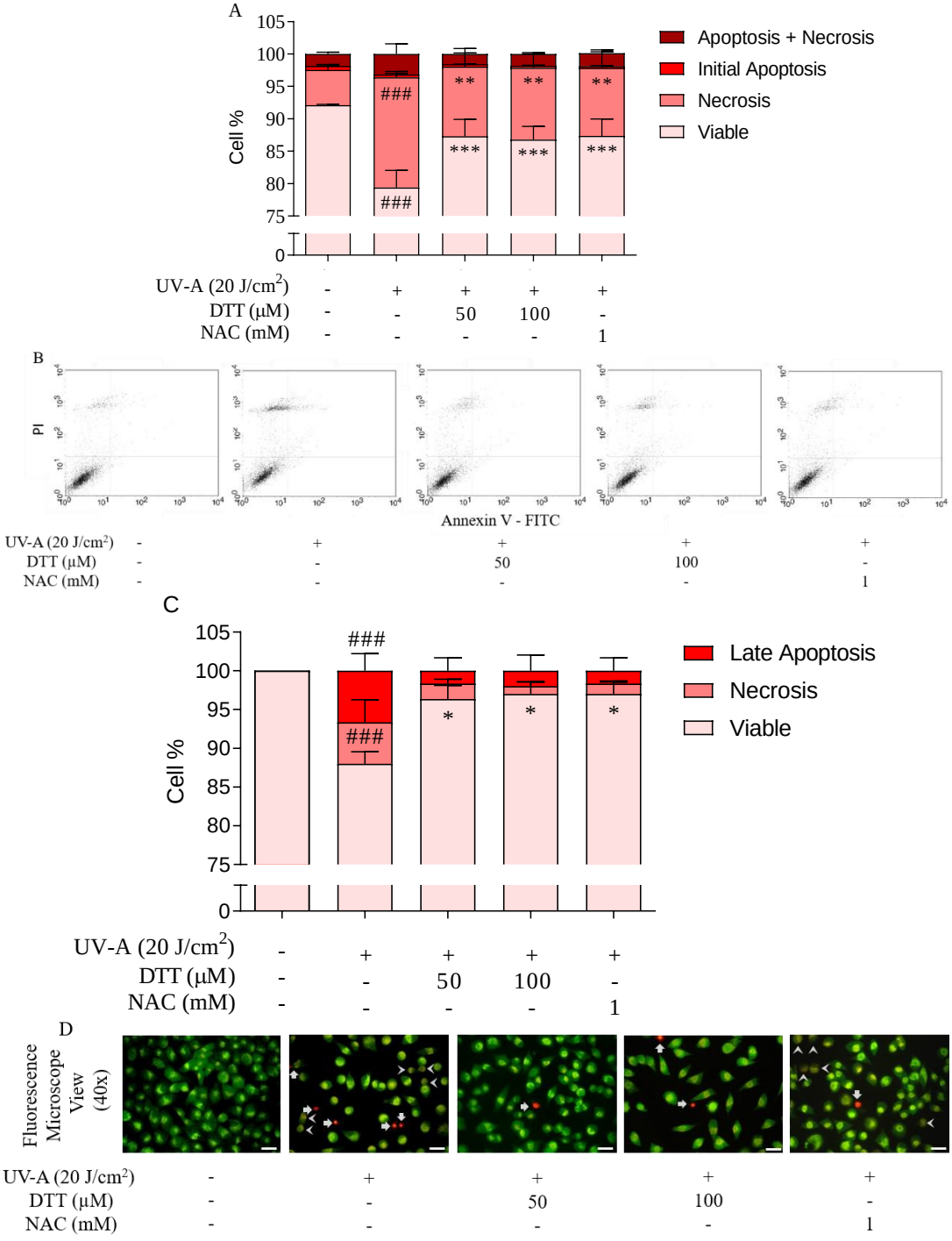

Figure 7. Effect of UV-A radiation (20 J/cm^2) and pre-treatment for 1 h with DTT on cell death of L929 fibroblasts. A and B: Evaluation of necrosis, initial apoptosis, necrosis + apoptosis and necrosis by flow cytometry using double-staining with Annexin V- FITC; C: Quantification of necrosis and apoptosis using double-staining acridine orange and propidium iodide from fluorescence microscopy images (D); D: White arrows indicate necrotic cells and arrow heads indicate late apoptotic cells. Each column represents the mean ± SD (n = 3). ### (p <0.001) indicates a significant difference compared to non-irradiated cells (first column). *, ** and *** (p < 0.05, p < 0.01 and p <0.001, respectively) indicates a

significant difference compared to cells irradiated with UV-A (second column) only. Each image represents three different experiments. Scale bars: 100 μm.

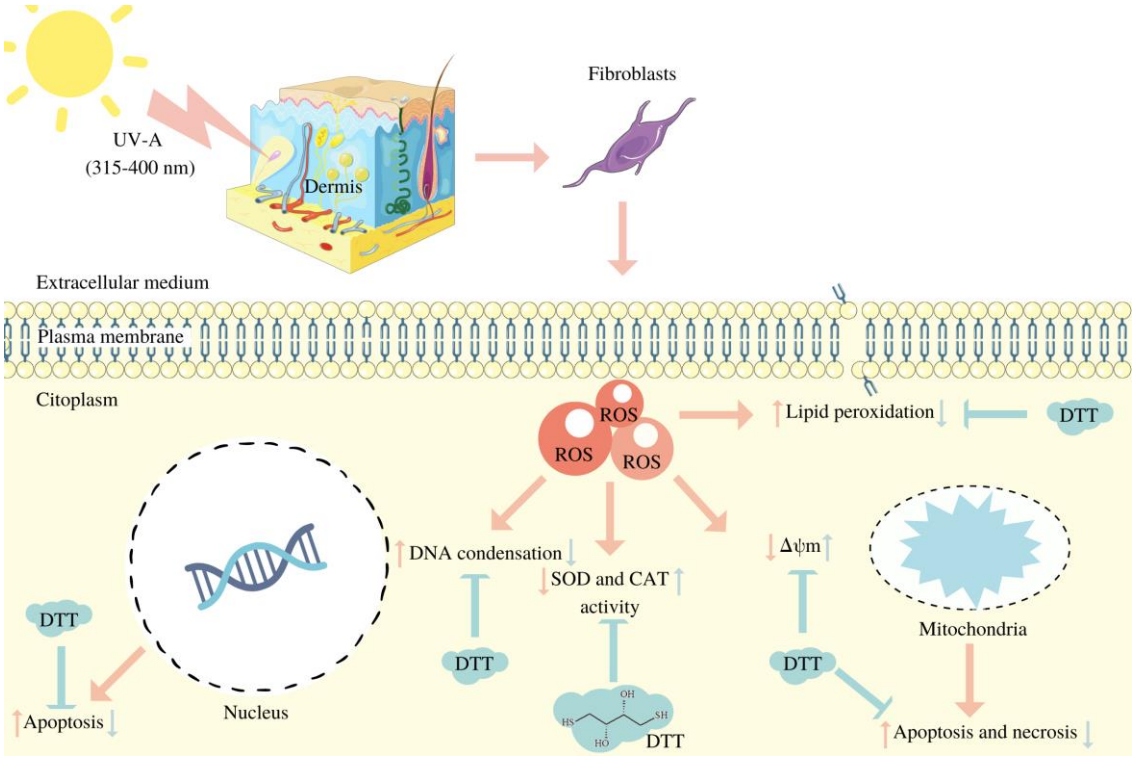

Figure 8. UV-A radiation (20 J/cm2) induces oxidative stress in L929 fibroblasts (red arrows) by increasing the production of ROS, which causes a decrease in the activity of antioxidant enzymes SOD and CAT, an increase in lipid peroxidation and depolarization of Δψm, leading to apoptosis and necrosis, as well as DNA condensation, leading to apoptosis. The blue arrows indicate the photochemoprotection of DTT, that acts against oxidative stress and cell death caused by UV-A radiation, for increase activity of SOD and CAT, reduction in lipid peroxidation, maintence of Δψm and reduction in DNA condensation, decreasing apoptosis and necrosis.

4. Conclusion

In summary, the results demonstrated that DTT has antioxidant activity capable of reducing oxidative stress that L929 fibroblasts are submitted when irradiated with UV-A. The pre-treatment of the cells with DTT promoted a photochemoprotection, since it reestablished in part the activity of the endogenous antioxidant system, attenuate ROS levels, including H_2O_2, reduce lipid peroxidation, condensation in the DNA and loss of Δψm. Cell death induced by exposure to UV-A radiation, both apoptosis and necrosis, was also reduced after DTT pre-treatment.

Data Available

The authors declare that all data used for the preparation of Tables and Figures are available.

CRediT Author Statement

Renata Bufollo Rodrigues: Conceptualization, methodology, validation, formal analysis, investigation, data curation and writing – original draft. Mariana Maciel de Oliveira: Methodology, writing – review and editing, project administration. Tânia Ueda-Nakamura: Supervision and funding acquisition. Sueli de Oliveira Silva: Supervision and funding acquisition. Celso Vataru Nakamura: writing – review and editing, supervision, project administration and funding acquisition.

Declaration of Competing Interest

All the authors declare no conflicts of interest.

Acknowledgements

To Capacitação de Aperfeiçoamento de Pessoal de Nível Superior (CAPES), Conselho Nacional de Desenvolvimento Científico e Tecnológico (CNPq), Financiadora de Estudos e Projetos (FINEP) and Programa de Apoio a Núcleos de Excelência (PRONEX/Fundação Araucária) for financial support during this project. To Complexo de Centrais de Apoio à Pesquisa (COMCAP/UEM) for structure and equipment support.

5. References

[1] J.M. Wierzbicka, M.A. Żmijewski, A. Piotrowska, B. Nedoszytko, M. Lange, R.C. Tuckey, A.T. Slominski, Bioactive forms of vitamin D selectively stimulate the skin analog of the hypothalamus-pituitary-adrenal axis in human epidermal keratinocytes, Mol. Cell. Endocrinol. 437 (2016) 312–322. https://doi.org/10.1016/j.mce.2016.08.006.

[2] R. Naffa, C. Maidment, M. Ahn, B. Ingham, S. Hinkley, G. Norris, Molecular and structural insights into skin collagen reveals several factors that influence its architecture, Int. J. Biol. Macromol. 128 (2019) 509–520. https://doi.org/10.1016/j.ijbiomac.2019.01.151.

[3] N. Yadav, M. Banerjee, Epidemiological aspects of photocarcinogenesis, Photocarcinogenes. Photoprotection. (2018) 53–63. https://doi.org/10.1007/978-981-10-5493-8_6.

[4] C. Battie, S. Jitsukawa, F. Bernerd, S. Del Bino, C. Marionnet, M. Verschoore, New insights in photoaging, UVA induced damage and skin types, Exp. Dermatol. 23 (2014) 7–12. https://doi.org/10.1111/exd.12388.

[5] R.S. Ray, C. Haldar, A. Dwivedi, N. Agarwal, J. Singh, Photocarcinogenesis and photoprotection (2018) 1–177. https://doi.org/10.1007/978-981-10-5493-8.

[6] J. Reichrath, The challenge resulting from positive and negative effects of sunlight: How much solar UV exposure is appropriate to balance between risks of vitamin D deficiency and skin cancer?, Prog. Biophys. Mol. Biol. 92 (2006) 9–16. https://doi.org/10.1016/j.pbiomolbio.2006.02.010.

[7] Q. Li, D. Wang, D. Bai, C. Cai, J. Li, C. Yan, S. Zhang, Z. Wu, J. Hao, G. Yu. Photoprotective effect of Astragalus membranaceus polysaccharide on UVA-induced damage in HaCaT cells, Plos One. 15 (2020) 1-14. https://doi.org/10.1371/journal.pone.0235515.

[8] A. Parzonko, A.K. Kiss, Caffeic acid derivatives isolated from Galinsoga parviflora herb protected human dermal fibroblasts from UVA-radiation, Phytomedicine. 57 (2019) 215–222. https://doi.org/10.1016/j.phymed.2018.12.022

[9] A.R. Young, J. Claveau, A.B. Rossi, Ultraviolet radiation and the skin: Photobiology and sunscreen photoprotection, J. Am. Acad. Dermatol. 76 (2017) 100–109. https://doi.org/10.1016/j.jaad.2016.09.038.

[10] D.G. Yeager, H.W. Lim, What's New in Photoprotection: A Review of New Concepts and Controversies, Dermatol. Clin. 37 (2019) 149–157. https://doi.org/10.1016/j.det.2018.11.003.

[11] L. Liu, J.R. Trimarchi, D.L. Keefe, Thiol Oxidation-Induced Embryonic Cell Death in Mice Is Prevented by the Antioxidant Dithiothreitol. 61 (1999) 1162-1169. https://doi.org/10.1095/biolreprod61.4.1162.

[12] L.C. Harber, J.M.D. Hsu, H.M.S. Hsu, B.D. Goldstein. Studies of Photoprotection Against Porphyrin Photosensibilization Usind Dithiothreitol and Glycerol. The Journal of Investigative Dermatology, 58 (1972) 373-380. https://doi.org/10.1111/1523-1747.ep12540600.

[13] DL-Dithiothreitol, (2016). http://www.cfmot.de/en/dl-dithiothreitol-dtt-biotech-grade.html (accessed January 15, 2021).

[14] R. Re, N. Pellegrini, A. Proteggente, A. Pannala, M. Yang, C. Rice-Evans, Antioxidant activity applying an improved ABTS radical cation decolorization assay, Free Radic. Biol. Med. 26 (1999) 1211–1237. https://doi.org/10.1016/S0891-5849(98)00315-3.

[15] M.S. Blois, Antioxidant determinations by the use of a stable free radical, Nature. 181 (1958) 1199–1200. https://doi.org/10.1038/1811199a0.

[16] M.M. Oliveira, B.A. Ratti, R.G. Daré, S.O. Silva, M.D.C.T. Truiti, T. Ueda-Nakamura, R. Auzély-Velty, C. V. Nakamura, Dihydrocaffeic acid prevents UVB-induced oxidative stress leading to the inhibition of apoptosis and MMP-1 expression via p38 signaling pathway, Oxid. Med. Cell. Longev. 2019 (2019). https://doi.org/10.1155/2019/2419096.

[17] S.H. Nile, A.S. Nile, Y.S. Keum, K. Sharma, Utilization of quercetin and quercetin glycosides from onion (*Allium* cepa L.) solid waste as an antioxidant, urease and xanthine oxidase inhibitors, Food Chem. 235 (2017) 119–126. https://doi.org/10.1016/j.foodchem.2017.05.043.

[18] V. Mareček, A. Mikyška, D. Hampel, P. Čejka, J. Neuwirthová, A. Malachová, R. Cerkal, ABTS and DPPH methods as a tool for studying antioxidant capacity of spring barley and malt, J. Cereal Sci. 73 (2017) 40–45. https://doi.org/10.1016/j.jcs.2016.11.004.

[19] S. Girotti, F. Fini, E. Ferri, R. Budini, S. Piazzi, D. Cantagalli, Determination of superoxide dismutase in erythrocytes by a chemiluminescent assay, Talanta. 51 (2000) 685–692. https://doi.org/10.1016/S0039-9140(99)00332-X.

[20] R.O. de Souza, G. de A.D. Alves, A.L.S.A. Forte, F. Marquele-Oliveira, D.F. da Silva, H. Rogez, M.J.V. Fonseca, *Byrsonima crassifolia* extract and fraction prevent UVB-induced oxidative stress in keratinocytes culture and increase antioxidant activity on skin, Ind. Crops Prod. 108 (2017) 485–494. https://doi.org/10.1016/j.indcrop.2017.07.015.

[21] E. Borenfreund, J.A. Puerner, Toxicity determined in vitro by morphological alterations and neutral red absorption, Toxicol. Lett. 24 (1985) 119–124. https://doi.org/10.1016/0378-4274(85)90046-3.

[22] J. Mikuła-Pietrasik, A. Kuczmarska, B. Rubiś, V. Filas, M. Murias, P. Zieliński, K. Piwocka, K. Ksiazek, Resveratrol delays replicative senescence of human mesothelial cells via mobilization of antioxidative and DNA repair mechanisms, Free Radic. Biol. Med. 52 (2012) 2234–2245. https://doi.org/10.1016/j.freerad biomed. 2012.03.014.

[23] R.G. Daré, M.M. Oliveira, M.C.T. Truiti, C. V. Nakamura, V.F. Ximenes, S.O.S. Lautenschlager, Abilities of protocatechuic acid and its alkyl esters, ethyl and heptyl protocatechuates, to counteract UVB-induced oxidative injuries and photoaging in fibroblasts L929 cell line, J. Photochem. Photobiol. B Biol. 203 (2020). https://doi.org/10.1016/j.jphotobiol.2019.111771.

[24] R. Patel, L. Rinker, J. Peng, W.M. Chilian, Reactive Oxygen Species: The Good and the Bad, React. Oxyg. Species Living Cells. (2018). https://doi.org/10.5772/intechopen.71547.

[25] J. Čapek, M. Hauschke, L. Brůčková, T. Roušar, Comparison of glutathione levels measured using optimized monochlorobimane assay with those from ortho-phthalaldehyde assay in intact cells, J. Pharmacol. Toxicol. Methods. 88 (2017) 40–45. https://doi.org/10.1016/j.vascn.2017.06.001.

[26] D.W.M. Walsh, C. Siebenwirth, C. Greubel, K. Ilicic, J. Reindl, S. Girst, G. Muggiolu, M. Simon, P. Barberet, H. Seznec, H. Zischka, G. Multhoff, T.E. Schmid, G. Dollinger, Live cell imaging of mitochondria following targeted irradiation in situ reveals rapid and highly localized loss of membrane potential OPEN, (2017). https://doi.org/10.1038/srep46684.

[27] V. Kaplum, A.C. Ramos, M.E.L. Consolaro, M.A. Fernandez, T. Ueda-Nakamura, B.P. Dias-Filho, S. de O. Silva, J.C.P. de Mello, C. V. Nakamura, Proanthocyanidin polymer-rich fraction of *Stryphnodendron adstringens*

promotes in vitro and in vivo cancer cell death via oxidative stress, Front. Pharmacol. 9 (2018) 1–18. https://doi.org/10.3389/fphar.2018.00694.

[28] M. Morita, Y. Naito, T. Yoshikawa, E. Niki, Plasma lipid oxidation induced by peroxynitrite, hypochlorite, lipoxygenase and peroxyl radicals and its inhibition by antioxidants as assessed by diphenyl-1-pyrenylphosphine, Redox Biol. 8 (2016) 127–135. https://doi.org/10.1016/j.redox.2016.01.005.

[29] J. Zheng, M.J. Piao, K.C. Kim, C.W. Yao, J.W. Cha, J.H. Shin, S.J. Yoo, J.W. Hyun, Photo-protective effect of americanin B against ultraviolet B-induced damage in cultured human keratinocytes, Environ. Toxicol. Pharmacol. 38 (2014) 891–900. https://doi.org/10.1016/j.etap.2014.08.017.

[30] D.R. Green, F. Llambi, Cell death signaling, Cold Spring Harb. Perspect. Biol. 7 (2015). https://doi.org/10.1101/cshperspect.a006080.

[31] Y. Tsujimoto, Apoptosis and necrosis: Intracellular ATP level as a determinant for cell death modes, Cell Death Differ. 4 (1997) 429–434. https://doi.org/10.1038/sj.cdd.4400262.

[32] S. Salucci, S. Burattini, D. Curzi, F. Buontempo, A.M. Martelli, G. Zappia, E. Falcieri, M. Battistelli, Antioxidants in the prevention of UVB-induced keratynocyte apoptosis, J. Photochem. Photobiol. B Biol. 141 (2014) 1–9. https://doi.org/10.1016/j.jphotobiol.2014.09.004.

[33] M. Gordeziani, G. Adamia, G. Khatisashvili, G. Gigolashvili, Programmed cell self-liquidation (apoptosis), Ann. Agrar. Sci. 15 (2017) 148–154. https://doi.org/10.1016/j.aasci.2016.11.001.

[34] H.W. Lim, M.I. Arellano-Mendoza, F. Stengel, Current challenges in photoprotection, J. Am. Acad. Dermatol. 76 (2017) S91–S99. https://doi.org/10.1016/j.jaad.2016.09.040.

[35] L. Duque, K. Bravo, E. Osorio, A holistic anti-aging approach applied in selected cultivated medicinal plants: A view of photoprotection of the skin by different mechanisms, Ind. Crops Prod. 97 (2017) 431–439. https://doi.org/10.1016/j.indcrop.2016.12.059.

[36] W.W. Cleland, Dithiothreitol, a New Protective Reagent for SH Groups, Biochemistry. 3 (1964) 480–482. https://doi.org/10.1021/bi00892a002.

[37] Y.S. T. Matsui, Y. Kitagawa, M. Okumura, Accurate Standard Hydrogen Electrode Potential and Applications to the Redox Potentials of Vitamin C and NAD/NADH, J. Phys. Chem. A. 119 (2014) 369–376. https://doi.org/10.1021/jp508308y.

[38] A.G.J. den Hartog, A.W. Boots , A. Adam-Perrot, F. Brouns, I. W. Verkooijen, A.R. Weseler, G.R. Haenen, Erythritol is a sweet antioxidant, Nutrition. 26 (2010) 449–458. https://doi.org/10.1016/j.nut.2009.05.004.

[39] R.C. Romanhole, J.A. Ataide, P. Moriel, P.G. Mazzola, Update on ultraviolet A and B radiation generated by the sun and artificial lamps and their effects on skin, Int. J. Cosmet. Sci. 37 (2015) 366–370. https://doi.org/10.1111/ics.12219.

[40] N.C. Moreno, C.C.M. Garcia, V. Munford, C.R.R. Rocha, A.L. Pelegrini, C. Corradi, A. Sarasin, C.F.M. Menck, The key role of UVA-light induced oxidative

stress in human Xeroderma Pigmentosum Variant cells, Free Radic. Biol. Med. 131 (2019) 432–442. https://doi.org/10.1016/j.freeradbiomed.2018.12.012.

[41] D.L. Nelson, M.M. Cox, Lehninger Principles of Biochemistry. 6th ed, New York. (2017) 47-69.

[42] L. Galluzzi, I. Vitale, Molecular mechanisms of cell death: recommendations of the Nomenclature Committee on Cell Death 2018, Cell Death Differ. 25 (2018) 486–541. https://doi.org/10.1038/s41418-017-0012-4.

[43] R.G. Daré, C. V. Nakamura, V.F. Ximenes, S.O.S. Lautenschlager, Tannic acid, a promising anti-photoaging agent: Evidences of its antioxidant and anti-wrinkle potentials, and its ability to prevent photodamage and MMP-1 expression in L929 fibroblasts exposed to UVB, Free Radic. Biol. Med. 160 (2020) 342–355. https://doi.org/10.1016/j.freeradbiomed.2020.08.019.

[44] C.C.E. Lan, P.Y. Ho, C.S. Wu, R.C. Yang, H.S. Yu, LED 590nm photomodulation reduces UVA-induced metalloproteinase-1 expression via upregulation of antioxidant enzyme catalase, J. Dermatol. Sci. 78 (2015) 125–132. https://doi.org/10.1016/j.jdermsci.2015.02.018.

[45] A. Narayanankutty, J.T. Job, V. Narayanankutty, Glutathione, an Antioxidant Tripeptide: Dual Roles in Carcinogenesis and Chemoprevention, Curr. Protein Pept. Sci. 20 (2019) 907–917. https://doi.org/10.2174/1389203720666190206130003.

[46] J. Van Der Paal, E.C. Neyts, C.C.W. Verlackt, A. Bogaerts, Effect of lipid peroxidation on membrane permeability of cancer and normal cells subjected to oxidative stress †, (2016). https://doi.org/10.1039/c5sc02311d.

[47] R. Karthikeyan, G. Kanimozhi, N.R. Prasad, B. Agilan, M. Ganesan, G. Srithar, Alpha pinene modulates UVA-induced oxidative stress, DNA damage and apoptosis in human skin epidermal keratinocytes, Life Sci. 212 (2018) 150–158. https://doi.org/10.1016/j.lfs.2018.10.004.

[48] L. Xiao, M. Mochizuki, T. Nakahara, N. Miwa, Hydrogen-generating silica material prevents uva-ray-induced cellular oxidative stress, cell death, collagen loss and melanogenesis in human cells and 3d skin equivalents, Antioxidants. 10 (2021) 1–16. https://doi.org/10.3390/antiox10010076.